Light-induced anthocyanin biosynthesis in Lilium brownii is mediated by the LbrHY5–LbrMYB6 module

Yuwei Cao

caoyw@gnnu.edu.cn

GanNan Normal University

Yuqian Zhang

GanNan Normal University

Huiwen Yang

GanNan Normal University

Yuwen Ye

GanNan Normal University

Hui Lai

GanNan Normal University

Shanghui Yin

GanNan Normal University

Wei Zhang

GanNan Normal University

Huyue Li

GanNan Normal University

Research Article

Keywords: Lilium brownii, Light signaling, LbrHY5, Anthocyanin biosynthesis, Transcriptional regulation, LbrMYB6

Posted Date: April 10th, 2026

DOI: https://doi.org/10.21203/rs.3.rs-9289041/v1

Additional Declarations: No competing interests reported.

Abstract

Lilium brownii is a valuable monocotyledonous plant with ornamental and medicinal importance, whose purplish-red pigmentation is attributed to anthocyanin accumulation under light exposure. However, the molecular mechanisms underlying light-regulated anthocyanin biosynthesis in lily remain unclear. Here, we demonstrate that light significantly enhances anthocyanin content in lily and upregulates key structural and LbrMYB6 regulatory genes. We identified LbrHY5 as a light-induced bZIP transcription factor localized to the nucleus. Transcriptomic analysis positioned LbrHY5 and LbrMYB6 at the central hubs of a light-responsive co-expression network. Moreover, molecular assays confirmed that LbrHY5 binds directly to the G-box motifs in promoters of LbrCHS and LbrMYB6, thereby activating their transcription. Overexpression of LbrHY5 and LbrMYB6 significantly increased anthocyanin accumulation and structural genes expression, with co-overexpression exhibiting synergistic effects. VIGS-mediated silencing of LbrMYB6 reduced anthocyanin contents and structural genes expression, while simultaneous silencing of both genes produced similar downregulation. Notably, individual silencing of LbrHY5 unexpectedly increased anthocyanin accumulation, suggesting complex regulatory mechanisms involving light-induced COP1 inactivation and potential feedback regulation. Collectively, our findings elucidated the role of a novel LbrHY5–LbrMYB6 module that mediates light-regulated anthocyanin biosynthesis in L. brownii, providing significant insights into the regulatory networks controlling pigmentation in monocots and offering potential strategies for improving color traits in ornamental lilies.

Key message

The LbrHY5–LbrMYB6 transcriptional module mediates light-induced anthocyanin biosynthesis in *Lilium brownie* by directly activating *LbrCHS* and downstream structural genes.

1 Introduction

Lilium brownii is a monocotyledonous plant with considerable ornamental, edible, and medicinal value. The purplish-red pigments in its floral organs and bulbs are primarily anthocyanins, which are flavonoids that contribute to pollination, stress resistance, and human health (Grotewold, 2006). Anthocyanin biosynthesis is controlled by both developmental programs and environmental cues, with light being one of the most influential factors (Winkel-Shirley, 2001).

Light represents a primary environmental determinant of anthocyanin accumulation across the plant kingdom. In dicotyledonous crops including tomato (*Solanum lycopersicum*) and grape (*Vitis vinifera*), light exposure coordinately induces expression of the core flavonoid biosynthetic genes—*PAL*, *CHS*, *F3H*, *DFR*, *ANS*, and *UFGT*—thereby promoting pigment synthesis in reproductive and vegetative tissues (Matus et al., 2009; Kim et al., 2021). Similarly, light exposure enhances the expression of anthocyanin-related genes in *Chrysanthemum morifolium* (Hong et al., 2016) and *Lilium regale* (Yamagishi, 2016), underscoring the conserved nature of light responses across species (Wei et al., 2011; Zhang et al., 2018; Zhou et al., 2022).

Among the central regulators mediating light signal transduction, ELONGATED HYPOCOTYL5 (HY5)—a bZIP transcription factor—stands out for its light-dependent accumulation and subsequent activation of genes governing photomorphogenesis and flavonoid metabolism (Feng et al., 2013; Wang et al., 2021). Under light, HY5 accumulates and binds to G-box or ACE-box elements in the promoters of target genes in the anthocyanin pathway, thereby activating transcription (Bursch et al., 2021; Liu et al., 2019; Maier et al., 2013).

Loss-of-function mutations in *HY5* have been linked to reduced pigmentation and transcriptional suppression of core anthocyanin biosynthetic genes in model species such as *Arabidopsi* and tomato (Li et al., 2018; Qiu et al., 2019; Wang et al., 2021). HY5 often functions alongside other factors, such as B-box (BBX) proteins and MYB transcription factors, forming complexes that fine-tune anthocyanin biosynthesis in response to light quality and intensity (Bai et al., 2019a; Fang et al., 2019; An et al., 2020). For example, PpHY5 and PpBBX16 form a complex that can binds directly to the *PpCHS* or *PpMYB10* promoter (Bai et al., 2019a). Additionally, HY5 stability is post-transcriptionally regulated by CONSTITUTIVELY PHOTOMORPHOGENIC 1 (COP1), which targets HY5 for degradation in darkness. Upon illumination, photoreceptors inhibit COP1, allowing HY5 to accumulate and bind to promoter elements of anthocyanin-related genes (Maier et al., 2013; Bursch et al., 2021).

MYB6, a key R2R3-MYB transcription factor, participate in light signal-mediated secondary metabolism across diverse plant species, particularly playing a critical role in the flavonoid and anthocyanin biosynthetic pathways. In *C. morifolium*, CmMYB6 functions as a central activator of anthocyanin biosynthesis and floral pigmentation (Xia et al., 2026). In *Populus tomentosa*, MYB6 positively regulates the accumulation of both anthocyanins and proanthocyanidins (PAs) (Wang et al., 2019). Similarly, in Sanhua plum's flesh (*Prunus salicina*), MYB6 is associated with *C4H* expression and anthocyanin accumulation (Xiang et al., 2023). Moreover, MYB6 transcription factors consistently show positive responsiveness to light signals. In *Fagopyrum tataricum*, the FtMYB6 promoter displays strong light-inducible activity, and its overexpression significantly enhances flavonol accumulation in transgenic tobacco and hairy roots of tartary buckwheat (Yao et al., 2020). However, LhMYB6 has been implicated in lily tepal pigmentation, and the mechanistic basis of its involvement in light-regulated anthocyanin biosynthesis remains elusive.

Although lily is a shade-loving plant, the mechanism underlying its flower coloration, especially its rich and bright colors in high-altitude areas with strong ultraviolet radiation, depends on the light signaling pathway. The role of HY5 has been extensively characterized in dicots, but its function in monocots, especially ornamental species (e.g., lily), remains poorly understood. *L. brownii* exhibits light-dependent pigmentation, but the regulatory network controlling this process has not been comprehensively elucidated. In this study, we functionally characterized LbrHY5 in terms of its role in light-induced anthocyanin biosynthesis. We determined that LbrHY5 is a nuclear protein that binds to the promoters of key anthocyanin-related genes. The target genes of LbrHY5, *LbrMYB6* and *LbrCHS*, were identified by combining transcriptome analysis with TF-centered Y1H screening. Moreover, *LbrHY5* and *LbrMYB6* overexpression can enhance pigment accumulation. Our results provide the first evidence of the

regulatory effects of the LbrHY5–LbrMYB6 module on anthocyanin biosynthesis in lily, offering new insights into light-mediated coloration in monocots.

2 Materials and methods

2.1 Light treatment of lily scales

L. brownii bulbs were purchased from Wanzai County (Yichun, Jiangxi, China). Light treatment was performed under cool white fluorescent light at an intensity of 100 μmol·m^{-2}·s^{-1}, with a constant temperature of 22 ± 2°C. Scales in the darkness group (D) were kept in complete darkness under the same temperature. For the light-treated groups, scales were exposed to continuous light for 1 day (L1) or 2 days (L2), respectively. Each treatment and subsequent phenotypic analysis were completed using 48 scales.

2.2 Anthocyanin quantification and gene expression analysis

Anthocyanins were extracted from scales after treatment with different light. The absorbances of the extracts at 530 nm, 620 nm and 650 nm were measured using a UV-2600 spectrophotometer (Shimadzu, Japan). The anthocyanin content was calculated as 0.1 OD (unit×10^3 g·FW^{-1}), and the calculation method was OD = (A_{530} - A_{620}) − 0.1 × (A_{650} - A_{620}).

Following different light treatments, *L. brownii* scales were harvested for total RNA extraction, after which complementary DNA (cDNA) was synthesized via reverse transcription. Gene-specific quantitative real-time PCR (qRT-PCR) primers were designed according to non-conserved gene sequences, with *Lilyactin* used as the internal reference. A qRT-PCR analysis was performed using SYBR Green master mix and a CFX96 system (Bio-Rad, USA), with relative expression levels determined according to the $2^{-\Delta\Delta Ct}$ method.

2.3 Transcriptome sequencing and bioinformatic analysis

An Illumina platform was used for a transcriptome sequencing analysis of *L. brownii* scales following different light treatments (D, L1, and L2), with three biological replicates per treatment. After quality control and alignment steps, DEGs were identified. GO and KEGG pathway enrichment analyses were conducted to determine the biological functions of DEGs.

2.4 Function identification of *LbrHY5* in *L. brownii*

The full-length *LbrHY5* cDNA sequence was cloned via rapid amplification according to the transcriptome data. Conserved domains were predicted using the NCBI Conserved Domain Database. In addition, a phylogenetic tree was constructed using the neighbor-joining method and MEGA 11 software.

2.5 Subcellular localization analysis

To generate the LbrHY5-GFP fusion construct, the coding sequence of *LbrHY5* (excluding the termination codon) was ligated in-frame upstream of the GFP coding region within the pCAMBIA2300 backbone. The resulting plasmid was introduced into *Agrobacterium tumefaciens* GV3101, and bacterial suspensions were infiltrated into *Nicotiana benthamiana* leaves for transient expression assays. After 3 days, GFP fluorescence was observed using a laser scanning confocal microscope, with nuclei counterstained by mCherry.

2.6 TF-centered Y1H assay to identify target genes

The key light-induced transcription factor gene *LbrHY5* was inserted into the pGADT7 vector to construct the bait vector. A library of yeast cells containing candidate *cis*-motifs was screened. Positive clones were selected on SD/−Trp/−Leu/−His medium supplemented with 100 mM 3-AT and then sequenced.

2.7 Promoter cloning

The promoter sequences of *LbrCHS* and *LbrMYB6* were isolated using the Genome Walking Kit (Clotech, China). Putative *cis*-acting elements were identified using the PlantCARE database.

2.8 Dual-luciferase reporter assay

The promoters of *LbrCHS* and *LbrMYB6* were inserted into the pGreenII 0800-LUC vector, whereas the *LbrHY5* CDS was cloned into the pGreenII 62-SK expression vector. Agrobacterium suspensions harboring the promoter reporter and transcription factor effector constructs were combined at a 10:1 volumetric ratio prior to co-infiltration into *N. benthamiana* leaves. Luciferase activities were measured after 3 days and then the firefly luciferase: *Renilla* luciferase ratio was calculated to determine transcriptional activation. The strain containing the empty expression vector was mixed with the reporter strain as a negative control. The firefly luciferase: *Renilla* luciferase ratio was set to 1, and 10 biological replicates were prepared for each experiment.

2.9 EMSA detection

The *LbrHY5* CDS was inserted into the pET-22b(+) expression vector. Recombinant LbrHY5-HIS was produced in *Escherichia coli* cells and purified. A western blot was used to detect the purified recombinant protein. Biotin-labeled double-stranded oligonucleotides containing the wild-type or mutated G-box motif were used as EMSA probes. Binding reactions were analyzed using a native polyacrylamide gel, with shifts detected using a chemiluminescent EMSA kit (Beyotime, China).

2.10 Overexpression and phenotypic analysis

The *LbrHY5* CDS was incorporated into the pCAMBIA1305 plant transformation vector. The resulting recombinant plasmid was inserted into *A. tumefaciens* strain EHA105 cells for the transformation of ‘Robina’ lily tepals and *L. brownii* scales via vacuum injection. MMA resuspension buffer [4.43 g/L MS (without vitamins), 20 g/L sucrose, 1.95 g/L MES, 10 mM $MgCl_2$, 100 μM acetosyringone, and 10 μM paclobutrazol, pH 5.6] was adjusted for an OD_{600} of 1.0. Tissues transformed with EV were used as the

control. Anthocyanin accumulation and the expression of related genes were compared overexpression and control lines following light treatments.

2.11 VIGS-mediated infection of lily tepals

Using the previously established petal VIGS system in lily (Bi et al., 2023), we cloned the *LbrHY5* and *LbrMYB6* genes and inserted them into the pTRV2 vector. The recombinant vectors were transformed into *Agrobacterium tumefaciens* strain EHA105 competent cells and resuspended in MMA buffer to an OD_{600} of 1.0. The *Agrobacterium* suspensions containing the recombinant pTRV2 and pTRV1 were mixed at a 1:1 ratio and infiltrated into tepals using a 0.05 MPa vacuum infiltration method for 5 min at room temperature. A mixture of *Agrobacterium* suspensions containing empty pTRV2 and pTRV1 was used as the control for anthocyanin content and structural gene expression analyses.

2.12 Statistical analysis

All experiments were performed with at least three independent biological replicates. Data are presented as means ± standard error of the mean (SEM). Statistical analyses were performed using GraphPad Prism 9.0 (GraphPad Software, USA). For comparisons between two groups, Student's t-test was applied. For comparisons among multiple groups, ordinary one-way ANOVA was performed, followed by Dunnett's multiple comparisons test when comparing all groups to a single control group. Statistical significance was set at $p < 0.05$, $p < 0.01$, and $p < 0.001$, as indicated in the figures. Different letters or asterisks denote statistically significant differences as described in the figure legends.

3 Results

3.1 Light promotes anthocyanin accumulation and related genes expression *in L. brownii*

To clarify the effects of light on *L. brownii* bulb coloration, we exposed scales to light for different durations (no light, 1 day of light, and 2 days of light) (Fig. 1A). In *L. brownii* bulbs, the anthocyanin content was almost undetectable in darkness. However, anthocyanin accumulated significantly as the duration of the light treatment increased, demonstrating a clear positive correlation between light exposure duration and anthocyanin production (Fig. 1B).

To elucidate the molecular basis of this light-induced pigmentation, we analyzed the expression levels of key structural and regulatory genes involved in anthocyanin biosynthesis. Notably, *LbrCHS1*, *LbrCHIb*, *LbrF3H*, *LbrFLS*, *LbrDFR*, *LbrANS*, *LbrANR* and *LbrMYB6* expression levels were consistently upregulated in response to light (Fig. 1C). Collectively, these findings indicate that an exposure to light not only promotes anthocyanin accumulation in *L. brownii* but also enhances the expression of anthocyanin-related genes. To comprehensively identify key transcription factors involved in light-induced anthocyanin biosynthesis in *L. brownii*, we performed transcriptomic analysis on scales subjected to different light treatments (D, L1, L2).

3.2 Transcriptomic analysis reveals anthocyanin-related gene expression changes in response to light

To elucidate the global changes in gene transcription levels in light-treated lily plants, we performed a transcriptome sequencing analysis of scales exposed to different light conditions. As shown in Fig. 2 and Supplementary Fig. 1, a Gene Ontology (GO) enrichment analysis revealed that differentially expressed genes (DEGs) after 1- and 2-day light treatments were significantly enriched in biological processes related to anthocyanin biosynthesis and light responses (Fig. 2A), thereby confirming that light is a key environmental signal activating anthocyanin biosynthesis. A Kyoto Encyclopedia of Genes and Genomes (KEGG) pathway enrichment analysis further demonstrated that these DEGs were specifically associated with the anthocyanin biosynthesis pathway (Fig. 2B), reflecting the coordinated activation of the complete biosynthetic network by light. A Venn diagram-based analysis identified both unique and shared genes among comparison groups (Fig. 2C), indicating that light-induced transcriptional reprogramming is a dynamic and complex process. Furthermore, there were significantly more upregulated genes than downregulated genes after light treatments (Fig. 2D), implying that light mainly activated anthocyanin biosynthesis-related gene expression.

Furthermore, to investigate the key DEGs associated with anthocyanin biosynthesis and their regulatory networks, we selected 31 DEGs in KEGG pathways related to anthocyanin and flavonoid biosynthesis for further analyses. A subcluster matrix revealed the consistent expression pattern among these genes, with an initial increase followed by stabilization (Fig. 3A). To identify potential core regulators, we constructed a co-expression network of the 31 anthocyanin-related DEGs. Notably, *LbrHY5* and *LbrMYB6* were positioned at the central hubs of this network (Fig. 3B), suggesting that they function as key transcription factors governing the light-responsive anthocyanin regulatory network. Based on these transcriptomic results, we selected *LbrHY5* and *LbrMYB6* as candidate genes for further functional characterization. Additionally, a cluster heatmap confirmed the significant upregulation of anthocyanin biosynthesis structural genes, such as *CHS*, *DFR*, and *ANS*, after an exposure to light (Fig. 3C).

Figure 2 Transcriptome analysis of L. brownii scales exposed to darkness (D), 1 day of light (L1), and 2 days of light (L2). (A) Enriched GO terms related to anthocyanin biosynthesis and light among differentially expressed genes (DEGs) in the D, L1, and L2 groups. (B) Enriched KEGG pathways related to anthocyanin biosynthesis among DEGs in the D, L1, and L2 groups. (C) Venn diagram of the overlapping DEGs among the three groups. (D) Results of the statistical analysis of upregulated and downregulated genes in the three groups.

3.3 LbrHY5 is a light-induced nuclear-localized transcription factor

Given that *LbrHY5* was identified as a core transcription factor from the transcriptomic co-expression network (Fig. 3B), we next performed bioinformatics analysis to characterize its sequence features and

expression patterns. To clarify the biological function of LbrHY5 in *L. brownii*, we isolated and cloned the full-length *LbrHY5* sequence. The encoded protein was revealed to contain 154 amino acids, with a calculated molecular weight of 17.4 kDa and a theoretical isoelectric point of 9.91. Additionally, the 810 bp full-length *LbrHY5* sequence included a 464 bp coding sequence (CDS), 80 bp 5'- untranslated region (UTR), and 306 bp 3'-UTR.

LbrHY5 expression levels were significantly upregulated following an exposure to continuous light for 2 days (relative to the expression in darkness), suggesting that *LbrHY5* is a light-responsive gene (Fig. 4A). To analyze the subcellular localization of LbrHY5, the *LbrHY5* CDS with the termination codon removed was cloned and inserted into the pCAMBIA2300-eGFP vector to generate the *35S*::*LbrHY5-GFP* fusion construct, with *35S*::*GFP* serving as the control construct. The LbrHY5-GFP fusion protein was exclusively localized in the nucleus (Fig. 4B), which is consistent with the prediction that LbrHY5 is a transcription factor.

To explore evolutionary relationships, MEGA 7.0 software was used to construct a phylogenetic tree for LbrHY5 and published HY5s according to the neighbor-joining method (with 1,000 bootstrap replicates). According to the results of the phylogenetic analysis, LbrHY5 was grouped in the HY5 subfamily (Fig. 4C). Furthermore, an amino acid sequence alignment using DNAMAN confirmed that LbrHY5 contains a conserved bZIP HY5-like domain included in the NCBI Conserved Domain Database, making it a member of the bZIP transcription factor family (Fig. 4D).

Figure 4 Bioinformatics analysis of LbrHY5 in lily. (A) *LbrHY5* expression levels in darkness and under light. Scales were treated with darkness (D) or continuous light for 2 days (L2). Data are presented as the mean ± SEM (n = 3). Statistically significant differences were determined using Student's *t*-test (** $p < 0.01$). (B) Subcellular localization of the LbrHY5-GFP fusion protein, with GFP alone used as a negative control. Bar, 100 μm. (C) Neighbor-joining phylogenetic tree derived from deduced amino acid sequences of LbrHY5 and other reported HY5s. Numbers next to nodes are bootstrap values from 1,000 replications. Amino acid sequences were retrieved from GenBank databases. (D) Amino acid sequence alignment of LbrHY5 and other reported HY5s. The bZIP HY5-like domain is indicated by a black line.

3.4 LbrHY5 binds to multiple types of *cis*-elements

To identify the *cis*-elements targeted by the LbrHY5 transcription factor, we performed a transcription factor-centered yeast one-hybrid (TF-centered Y1H) assay. We first constructed the *LbrHY5* gene into the pGADT7 vector to generate the bait vector and then conducted a background screening test. As shown in Supplementary Fig. 2, yeast growth was undetectable at a concentration of 100 mM 3-AT, reflecting minimal auto-activation and validating the suitability of the system for library screening. The pGADT7-LbrHY5 bait vector was then transformed into a yeast library containing candidate *cis*-elements, with positive clones initially screened on SD/−Trp/−Leu/−His medium supplemented with 100 mM 3-AT. Selected clones were sequenced and analyzed using BLAST, which was following by a one-to-one verification of the confirmed clones. According to the results, LbrHY5 can bind to various *cis*-elements, including AT-rich motifs, CACT motifs, and RAV1-binding sites (Fig. 5A and Supplementary Table 1).

A combined analysis of transcriptome data and TF-centered Y1H assay results identified several potential targets of LbrHY5, including the key anthocyanin biosynthesis-related genes *LbrCHS* and *LbrMYB6*. We subsequently isolated their promoter sequences by genome walking, obtaining 764 bp and 680 bp fragments, respectively (Fig. 5B). Notably, using PlantCARE to examine *LbrCHS* and *LbrMYB6* promoter sequences, we detected the presence of various *cis*-elements, including AT-rich motifs, CACT motifs, RAV1-binding sites, and G-box elements (Fig. 5C).

3.5 LbrHY5 directly activates *LbrCHS* and *LbrMYB6* transcription

To confirm the direct binding of LbrHY5 to target gene promoters, we conducted a series of molecular assays. Considering the G-box element, which is a conserved promoter motif targeted by HY5, was detected in the *LbrCHS* and *LbrMYB6* promoters, we examined LbrHY5 in terms of its ability to bind to the G-box sequence. On the basis of an electrophoretic mobility shift assay (EMSA), purified LbrHY5 can bind specifically to *LbrCHS* and *LbrMYB6* promoter fragments containing the G-box motif (Fig. 6A and B). The specificity of this binding was confirmed by competition assays, in which protein–DNA interactions were effectively disrupted by an excess of unlabeled wild-type probe, but remained unaffected by a mutated probe. Hence, the G-box promoter element was identified as a binding site for LbrHY5.

Furthermore, to determine whether this binding leads to transcriptional activation, we performed a dual-luciferase (LUC) reporter assay using *N. benthamiana* leaves. Specifically, we constructed effector vectors expressing *LbrHY5* as well as reporter vectors for the expression of the firefly luciferase gene under the control of the *LbrCHS* or *LbrMYB6* promoter (Fig. 6C). Compared with the control, the co-expression of *LbrHY5* resulted in a significant increase in luciferase activity (Fig. 6D and E), indicating that LbrHY5 can directly activate *LbrCHS* and *LbrMYB6* transcription by binding to their promoters.

3.6 Overexpression of *LbrHY5-LbrMYB6* enhances anthocyanin biosynthesis

To explore the specific biological functions of *LbrHY5* and *LbrMYB6* in lily, we constructed the pCAMBIA1305-*LbrHY5* and pCAMBIA1305-*LbrMYB6* recombinant overexpression vector and inserted it into ‘Robina’ tepals. All transgenic plants were incubated in darkness for 2 days and then exposed to light for 1 day. Compared with EV ‘Robina’ tepals, the tepals of transgenic plants were more extensively colored (Fig. 7A) and had higher total anthocyanin contents (Fig. 7B). Additionally, key structural and regulatory genes in the anthocyanin biosynthesis pathway (*LbrCHS*, *LbrCHI*, *LbrDFR*, *LbrANS*, and *LbrMYB6*) were expressed at significantly higher levels in OE-*LbrHY5* transgenic tepals than in EV control tepals. Further analysis revealed that OE-*LbrMYB6* treatment also promoted the expression of these structural genes, and their expression levels were positively correlated with anthocyanin content. Notably, when *LbrHY5* and *LbrMYB6* were overexpressed simultaneously, the transcriptional levels of the structural genes were more significantly upregulated compared with either single overexpression

treatment, indicating a synergistic effect of these two factors in activating the transcription of structural genes (Fig. 7C). Considered together, these observations suggest that LbrHY5 and LbrMYB6 positively regulates anthocyanin biosynthesis in lily, enhancing pigment accumulation through the transcriptional activation of key structural and regulatory genes in the anthocyanin biosynthesis pathway. Notably, while co-overexpression of *LbrHY5* and *LbrMYB6* resulted in higher expression levels of structural genes compared with single overexpression (Fig. 7C), the total anthocyanin content in the co-overexpression group was slightly lower than that in the OE-*LbrMYB6* group (Fig. 7B). This discrepancy may be attributed to post-transcriptional regulatory mechanisms or rate-limiting steps in the anthocyanin biosynthetic pathway that are not fully reflected at the transcript level. Alternatively, excessive activation of the pathway by simultaneous overexpression of two strong activators might trigger feedback inhibition or metabolic flux redistribution, leading to attenuated anthocyanin accumulation.

3.7 Analysis of VIGS-mediated silencing of *LbrHY5* and *LbrMYB6*

To further validate the roles of *LbrHY5* and *LbrMYB6* in anthocyanin biosynthesis in lily, VIGS technology was employed to perform gene silencing in ‘Robina’ lily tepals. The results showed that, compared with the empty vector (pTRV1 + pTRV2) control, tepals with individual silencing of *LbrHY5* (pTRV1 + pTRV2-*LbrHY5*) exhibited significantly increased anthocyanin content (Fig. 8A and B), along with significantly upregulated expression levels of structural genes (*LbrCHS*, *LbrCHI*, *LbrDFR*, *LbrANS*) and *LbrMYB6* in the anthocyanin biosynthesis pathway (Fig. 8C).

In contrast to *LbrHY5* silencing, tepals with individual silencing of *LbrMYB6* (pTRV1 + pTRV2-*LbrMYB6*) and simultaneous silencing of both *LbrHY5* and *LbrMYB6* (pTRV1 + pTRV2-*LbrHY5* + pTRV2-*LbrMYB6*) showed significantly reduced anthocyanin content (Fig. 8B), and the expression levels of the structural genes were all significantly downregulated (Fig. 8C).

3.8 A Working model for the LbrHY5-mediated regulatory effects of light on anthocyanin biosynthesis

Based on our findings, we propose a comprehensive working model that elucidates the central role of LbrHY5 in light-induced anthocyanin biosynthesis in *L. brownii* (Fig. 9). Under dark conditions, *LbrHY5* transcription is maintained at low levels, resulting in minimal expression of its target genes *LbrCHS* and *LbrMYB6*, and consequently, low anthocyanin accumulation. Following an exposure to light, *LbrHY5* transcription is strongly activated. The LbrHY5 protein then directly binds to the G-box motifs in the promoters of *LbrCHS* (a key structural gene) and *LbrMYB6* (a regulatory transcription factor), activating their transcription. The upregulation of *LbrMYB6* further promotes the expression of downstream anthocyanin structural genes (*LbrCHS*, *LbrCHI*, *LbrDFR*, *LbrANS*), establishing a transcriptional cascade that amplifies the light signal. This coordinated activation of the anthocyanin biosynthetic pathway

ultimately leads to substantial anthocyanin accumulation and the characteristic pigmentation in lily scales. (Yamagish et al., 2010).

In summary, the synergistic effects of two processes (i.e., direct activation by LbrHY5 and amplified regulation via LbrMYB6) lead to a robust and coordinated upregulation of the anthocyanin biosynthesis pathway. The associated transcriptional cascade ultimately leads to substantial anthocyanin accumulation in lily, resulting in a characteristic red coloration.

4 Discussion

4.1 Light as a key environmental signal promoting anthocyanin biosynthesis in *Lilium brownii*

Light is an indispensable factor affecting plant coloration. Lily is a shade-loving plant that is highly sensitive to light. Insufficient light affects plant growth, while also influencing flower bud differentiation, resulting in flower and fruit drop. During the dicots of tomato (*S. lycopersicum*) and grape (*Vitis vinifera*), bags are often used to cover developing fruits, but they are removed to stimulate the rapid anthocyanin biosynthesis and accumulation at the mature stage. Moreover, the expression levels of anthocyanin biosynthesis-related structural genes (*PAL*, *CHS*, *CHI*, *F3H*, *DFR*, *ANS* and *UFGT*) are significantly upregulated after an exposure to light (Matus et al., 2009; Kim et al., 2021). In *C. morifolium*, anthocyanin biosynthesis genes (*CmCHS*, *CmF3H*, *CmANS*, *CmDFR* and *Cm3GT*) are reportedly expressed at lower levels in shaded plants than in plants exposed to normal light conditions (Hong et al., 2016). Another study showed that shading *L. regale* plants results in downregulated *LrCHSa*, *LrCHSb*, *LrF3H*, *LrF3'H*, *LrDFR* and *LrANS* expression levels, but the expression of anthocyanin biosynthesis genes is upregulated after light treatments, leading to increased tepal color formation (Yamagishi, 2016), which was consistent with the results of the current study. Our study demonstrates that an exposure to light significantly promotes anthocyanin accumulation in *L. brownii*, accompanied by the upregulation expression of structural and regulatory genes in anthocyanin pathway, including *LbrCHS*, *LbrCHIb*, *LbrF3H*, *LbrFLS*, *LbrDFR*, *LbrANS*, *LbrANR* and *LbrMYB6*.

4.2 Transcriptomic insights into the LbrHY5–LbrMYB6 co-regulatory network

Transcriptome profiling further revealed broad transcriptional reprogramming under light, emphasizing the role of LbrHY5 as a master regulator of the anthocyanin pathway. The induction of *LbrMYB6* expression by LbrHY5 reflects the potential crosstalk between light and stress signaling pathways because LbrMYB6 is a transcription factor that modulates flavonoid biosynthesis in response to environmental stimuli.

In conclusion, we propose a model in which light stabilizes LbrHY5, which in turn activates the expression of *LbrMYB6* and structural genes, such as *LbrCHS*, leading to anthocyanin accumulation in

lily. To the best of our knowledge, this study is the first to functionally characterize LbrHY5 in lily, which is a monocotyledonous ornamental species. The study data may form the theoretical basis for improving color traits in *L. brownii* via light treatment or genetic engineering, with implications for the optimizing *L. brownii*.

4.3 LbrHY5 functions as a central light-responsive transcription factor in lily

We identified LbrHY5 as a bZIP transcription factor localized in the nucleus, wherein it positively regulates anthocyanin biosynthesis. HY5, which is a well-known integrator of light signals in plants, is relatively stable under light and activates the expression of downstream target genes involved in photomorphogenesis and pigment synthesis (Chen et al., 2013; Wang et al., 2021). Earlier research showed that HY5 activates the transcription of anthocyanin biosynthesis structural genes in response to light signals by binding to the G-box element in target gene promoter regions (Chen et al., 2022; Liu et al., 2019). Under light conditions, HY5 promotes anthocyanin biosynthesis and accumulation in plants. Accordingly, deleting the *hy5* gene in plants leads to decreased anthocyanin contents. The positive regulatory role of HY5 in anthocyanin biosynthesis appears evolutionarily conserved across dicot species. In *Arabidopsis*, HY5 directly transactivates structural anthocyanin genes while also partnering with BBX proteins to amplify transcriptional output (Bursch et al., 2021). Similarly, in tomato, SlHY5 regulates the expression of *CHS*, *F3H*, *DFR*, *ANS*, and *3-GT* compared with wild-type controls, *hy5* mutants have lower anthocyanin contents (Qiu et al., 2019; Wang et al., 2021). In the present study, both *LbrHY5* and *LbrMYB6* overexpression increased anthocyanin levels and upregulated *LbrCHS*, *LbrCHI, LbrDFR* and *LbrANS* expression, suggesting that *LbrHY5* encodes a conserved positive regulator of anthocyanin accumulation. Moreover, VIGS silencing experiments confirmed these findings while revealing complex regulation of LbrHY5. Unexpectedly, individual silencing of *LbrHY5* significantly increased anthocyanin content and structural gene expression. This unexpected phenomenon may be attributed to complex regulatory feedback mechanisms. In many plant species, HY5 stability is post-translationally regulated by COP1 in darkness, and light exposure inactivates COP1, allowing HY5 accumulation (Zhao et al., 2022; Bi et al., 2025). Although similar mechanisms may operate in lily, further experiments are needed to elucidate the precise post-transcriptional regulation of LbrHY5 and the feedback responses triggered by partial silencing. Additionally, this partial silencing may have activated a feedback mechanism that enhances its own transcription, or directly increased anthocyanin biosynthesis via a compensatory upregulation of its target, *LbrMYB6*. However, co-silencing *LbrHY5* and *LbrMYB6* similarly downregulated anthocyanin-related genes, consistent with their synergistic effect observed in overexpression assays. Taken together, these findings suggest that LbrHY5 exhibits more complex regulation involving light signaling and potential feedback mechanisms.

4.4 Distinct regulatory mechanisms of LbrHY5 in lily compared to dicot models

Previous studies showed that HY5 regulates plant anthocyanin accumulation in response to light, and requires BBX factor to mediate and promote plant photomorphogenesis, but the regulatory mechanisms are different (Fang et al., 2019; Liu et al., 2022). In addition, studies have shown that HY5 can also regulate the transcriptional expression of downstream genes by interacting with MYB transcription factors and affecting the stability of MBW complex. The interaction between HY5 and MIR858a in *A. thaliana* promotes anthocyanin accumulation in seedlings, inhibits the expression of *MYBL2*, a negative regulator of anthocyanin biosynthesis, and activates the expression of anthocyanin biosynthesis structural genes in response to light signals (Wang et al., 2016). In pear, it was found that PpBBX16 cannot directly bind to the *PpCHS* or *PpMYB10* promoters, but the PpBBX16–PpHY5 complex can enhance the activity of MdMYB10 promoter (Bai et al., 2019a). Moreover, PpHY5 alone cannot activate the transcription of target genes, and inhibits *PpMYB10* expression with the help of PpBBX18 and PpBBX21, thereby regulating the biosynthesis of anthocyanin (Bai et al., 2019b). In apple calli, MdBBX22 binds to MdHY5 to form a complex that activates the anthocyanin biosynthesis pathway, ultimately promoting anthocyanin accumulation and coloration under UV-B light (Bai et al., 2014; An et al., 2019). Conversely, MdBBX37 suppresses anthocyanin accumulation by binding to the *MdHY5* promoter without interacting with the protein (An et al., 2020). Notably, in the current study, we determined that LbrHY5 can bind to the promoters of *LbrCHS* and *LbrMYB6* in yeast one-hybrid assays, although it did not interact with LbrMYB6 in yeast two-hybrid assays. This suggests that LbrHY5 may directly activate the expression of these genes without forming stable complexes with the encoded proteins. The lack of LbrHY5–LbrMYB6 interaction in lily may reflect species-specific regulatory mechanisms, with LbrHY5 functioning independently of LbrMYB6. This differs from the regulatory mechanism in pear and apple, wherein HY5 forms complexes with MYB or BBX. Hence, compared with other plants, lily may have a more direct transcriptional activation mechanism.

5 Conclusions

Our study provides a systematically regulatory mechanism of light-induced anthocyanin biosynthesis in *Lilium brownii*. We demonstrated that light exposure significantly promotes anthocyanin accumulation and upregulates the expression of key structural genes (*LbrCHS*, *LbrCHI*, *LbrF3H*, *LbrFLS*, *LbrDFR*, *LbrANS*, *LbrANR*) and the regulatory gene *LbrMYB6*. LbrHY5 was identified as a light-responsive bZIP transcription factor localized to the nucleus, with its expression significantly induced by light. Transcriptome analysis revealed that *LbrHY5* and *LbrMYB6* serve as central hubs in a light-responsive co-expression network regulating anthocyanin biosynthesis. Electrophoretic mobility shift and dual-luciferase reporter assays collectively demonstrated that LbrHY5 engages G-box *cis*-elements within the *LbrCHS* and *LbrMYB6* promoters, thereby driving their transcriptional activation. Functional analyses through overexpression and VIGS silencing demonstrated that both LbrHY5 and LbrMYB6 positively regulate anthocyanin biosynthesis, with synergistic effects observed upon co-overexpression. The unexpected increase in anthocyanin accumulation following individual *LbrHY5* silencing may be attributed to light-induced COP1 inactivation and potential feedback regulatory mechanisms. In conclusion, our findings establish that the LbrHY5–LbrMYB6 transcriptional module plays a critical role in mediating light-induced anthocyanin

biosynthesis in *L. brownii*, providing new insights into the regulatory networks controlling pigmentation in monocotyledonous plants and offering potential targets for genetic improvement of color traits in ornamental lilies.

Declarations

Declaration of competing interest

The authors declare that they have no known competing financial interests or personal relationships that could have appeared to influence the work reported in this paper.

Funding Declaration

This work was supported by the National Natural Science Foundation of China (32402611); Jiangxi Provincial Department of the National Natural Science Foundation (20232BAB215044) and Key Science and Technology Research Project in Jiangxi Province Department of Education (GJJ2201232).

Acknowledgments

This study was conducted at the Ganzhou Key Laboratory of Nanling Plant Resources Protection and Utilization and Jiangxi Provincial Key Laboratory of Pest and Disease Control of Featured Horticultural Plants, China.

Data availability

Data will be made available on request.

References

1. An JP, Wang XF, Espley RV, Lin-Wang K, Bi SQ, You CX, Hao YJ (2020) An apple B-box protein MdBBX37 modulates anthocyanin biosynthesis and hypocotyl elongation synergistically with MdMYBs and MdHY5. Plant Cell Physiol 61: 130–143
2. An JP, Wang XF, Zhang XW, Bi SQ, You CX, Hao YJ (2019) MdBBX22 regulates UV-B-induced anthocyanin biosynthesis through regulating the function of MdHY5 and is targeted by MdBT2 for 26S proteasome-mediated degradation. Plant Biotechnol J 17: 2231–2233
3. Bai SL, Saito T, Honda C, Hatsuyama Y, Ito A, Moriguchi T (2014) An apple B-box protein, MdCOL11, is involved in UV-B- and temperature-induced anthocyanin biosynthesis. Planta 240: 1051–1062
4. Bai SL, Tao RY, Tang YX, Yin L, Ma YJ, Ni JB, Yan XH, Yang QS, Wu ZY, Zeng YL, Teng YW (2019a) BBX16, a B-box protein, positively regulates light-induced anthocyanin accumulation by activating *MYB10* in red pear. Plant Biotechnol J 17: 1985–1997
5. Bai SL, Tao RY, Yin L, Ni JB, Yang QS, Yan XH, Yang F, Guo XP, Li HX, Teng YW (2019b) Two B-box proteins, PpBBX18 and PpBBX21, antagonistically regulate anthocyanin biosynthesis via

competitive association with *Pyrus pyrifolia* ELONGATED HYPOCOTYL 5 in the peel of pear fruit. Plant J 100: 1208–1223

6. Bi MM, Liang R, Wang J, Qu YX, Liu X, Cao YW, He GR, Yang Y, Yang PP, Xu LF, Ming J (2023) Multifaceted roles of LhWRKY44 in promoting anthocyanin accumulation in Asiatic hybrid lilies (*Lilium* spp.). Hortic Res 10: uhad167
7. Bi XY, Zhu YX, Fan JM, Zhang LX, Lin AQ, Wang C, Liu ZC, Zhang LQ, Kuang HY, Xu PB, Lian HL (2025) The E3 ubiquitin ligase COP1 inhibits sugar and anthocyanin accumulation in strawberry fruit. Plant Physiol 198: kiaf339
8. Bursch K, Niemann ET, Nelson DC, Johansson H (2021) Karrikins control seedling photomorphogenesis and anthocyanin biosynthesis through a HY5-BBX transcriptional module. Plant J 107: 1346–1362
9. Chen DQ, Xu G, Tang WJ, Jing YJ, Ji Q, Fei ZJ, Lin RC (2013) Antagonistic basic Helix-Loop-Helix/bZIP transcription factors form transcriptional modules that integrate light and reactive oxygen species signaling in *Arabidopsis*. Plant Cell 25: 1657–1673
10. Chen R, Yang C, Gao H, Shi CM, Zhang ZY, Lu GY, Shen XY, Tang YP, Li F, Lu YE, Ouyang B (2022) Induced mutation in ELONGATED HYPOCOTYL5 abolishes anthocyanin accumulation in the hypocotyl of pepper. Theor Appl Genet 135: 3455–3468
11. Fang HC, Dong YH, Yue XX, Hu JF, Jiang SH, Xu HF, Wang YC, Su MY, Zhang J, Zhang ZY, Wang N, Chen XS (2019) The B-box zinc finger protein MdBBX20 integrates anthocyanin accumulation in response to ultraviolet radiation and low temperature. Plant Cell Environ 42: 2090–2104
12. Feng FJ, Li MJ, Ma FW, Cheng LL (2013) Phenylpropanoid metabolites and expression of key genes involved in anthocyanin biosynthesis in the shaded peel of apple fruit in response to sun exposure. Plant Physiol Biochem 69: 54–61
13. Grotewold E (2006) The genetics and biochemistry of floral pigments. Annu Rev Plant Biol 57: 761–780
14. Hong Y, Yang LW, Li ML, Dai SL (2016) Comparative analyses of light-induced anthocyanin accumulation and gene expression between the ray florets and leaves in *chrysanthemum*. Plant Physiol Biochem 103: 120–132
15. Kim MJ, Kim P, Chen YZ, Chen BW, Yang JF, Liu X, Kawabata S, Wang Y, Li YH (2021) Blue and UV-B light synergistically induce anthocyanin accumulation by co-activating nitrate reductase gene expression in Anthocyanin fruit (*Aft*) tomato. Plant Biol 23: 210–220
16. Li J, He YJ, Zhou L, Liu Y, Jiang MM, Ren L, Chen HY (2018) Transcriptome profiling of genes related to light-induced anthocyanin biosynthesis in eggplant (*Solanum melongena* L.) before purple color becomes evident. BMC Genomics 19: 201
17. Liu HN, Su J, Zhu YF, Yao GF, Allan AC, Ampomah-Dwamena C, Shu Q, Lin-Wang K, Zhang SL, Wu J (2019) The involvement of *PybZIPa* in light-induced anthocyanin accumulation via the activation of *PyUFGT* through binding to tandem G-boxes in its promoter. Hortic Res 6: 134

18. Liu YQ, Ye YT, Wang YP, Jiang LY, Yue ML, Tang L, Jin MSX, Zhang YT, Lin YX, Tang HR (2022) B-box transcription factor FaBBX22 promotes light-induced anthocyanin accumulation in strawberry (*Fragaria* × *ananassa*). Int J Mol Sci 23: 7757
19. Maier A, Schrader A, Kokkelink L, Falke C, Welter B, Iniesto E, Rubio V, Uhrig JF, Hulskamp M, Hoecker U (2013) Light and the E3 ubiquitin ligase COP1/SPA control the protein stability of the MYB transcription factors PAP1 and PAP2 involved in anthocyanin accumulation in Arabidopsis. Plant J 74: 638–651
20. Matus JT, Loyola R, Vega A, Pena-Neira A, Bordeu E, Arce-Johnson P, Alcalde JA (2009) Post-veraison sunlight exposure induces MYB-mediated transcriptional regulation of anthocyanin and flavonol synthesis in berry skins of *Vitis vinifera*. J Exp Bot 60: 853–867
21. Qiu ZK, Wang HJ, Li DJ, Yu BW, Hui QL, Yan SS, Huang ZJ, Cui X, Cao BH (2019) Identification of candidate HY5-dependent and -independent regulators of anthocyanin biosynthesis in tomato. Plant Cell Physiol 60: 643–656
22. Wang LJ, Lu WX, Ran LY, Dou LW, Yao S, Hu J, Fan D, Li CF, Luo KM (2019) R2R3-MYB transcription factor MYB6 promotes anthocyanin and proanthocyanidin biosynthesis but inhibits secondary cell wall formation in *Populus tomentosa*. Plant J 99: 733–751
23. Wang WH, Wang PW, Li XJ, Wang YY, Tian SP, Qin GZ (2021) The transcription factor SlHY5 regulates the ripening of tomato fruit at both the transcriptional and translational levels. Hortic Res 8: 83
24. Wang YL, Wang YQ, Song ZQ, Zhang HY (2016) Repression of *MYBL2* by both microRNA858a and HY5 leads to the activation of anthocyanin biosynthetic pathway in *Arabidopsis*. Mol Plant 9: 1395–1405
25. Wei YZ, Hu FC, Hu GB, Li XJ, Huang XM, Wang HC (2011) Differential expression of anthocyanin biosynthetic genes in relation to anthocyanin accumulation in the pericarp of *Litchi chinensis* Sonn. PLoS One 6: e19455
26. Winkel-Shirley B (2001) It takes a garden. How work on diverse plant species has contributed to an understanding of flavonoid metabolism. Plant Physiol 127: 1399–1404
27. Xia WH, Wang YX, Zhao G, Peng JL, Li XG, Li YK, Tian YH, Song AP, Chen SM, Chen FD, Zhou LJ (2026) Genome-wide identification of MYC transcription factors in *Chrysanthemum morifolium* and CmMYC25 promotes petal anthocyanin accumulation. Plant Cell Rep 45: 33
28. Xiang N, Chang XX, Qin LW, Li K, Wang SY, Guo XB (2023) Insights into tissue-specific anthocyanin accumulation in Japanese plum (*Prunus salicina* L.) fruits: A comparative study of three cultivars. Food Chem Mol Sci 7: 100178
29. Yamagishi M, Shimoyamada Y, Nakatsuka T, Masuda K (2010) Two *R2R3-MYB* genes, homologs of Petunia *AN2*, regulate anthocyanin biosyntheses in flower tepals, tepal spots and leaves of Asiatic hybrid lily. Plant Cell Physiol 51: 463–474
30. Yamagishi M (2016) A novel R2R3-MYB transcription factor regulates light-mediated floral and vegetative anthocyanin pigmentation patterns in *Lilium regale*. Mol Breed 36: 3

31. Yao PF, Huang YJ, Dong QX, Wan M, Wang AH, Chen YW, Li CL, Wu Q, Chen H, Zhao HX (2020) FtMYB6, a light-induced SG7 R2R3-MYB transcription factor, promotes flavonol biosynthesis in tartary buckwheat (*Fagopyrum tataricum*). J Agric Food Chem 68: 13685–13696
32. Zhang YZ, Xu SZ, Cheng YW, Peng ZF, Han JM (2018) Transcriptome profiling of anthocyanin-related genes reveals effects of light intensity on anthocyanin biosynthesis in red leaf lettuce. PeerJ 6: e4607
33. Zhao L, Sun JL, Cai YM, Yang QR, Zhang YQ, Ogutu CO, Liu JJ, Zhao Y, Wang FR, He HP, Zheng BB, Han YP (2022) PpHYH is responsible for light-induced anthocyanin accumulation in fruit peel of *Prunus persica*. Tree Physiol 42: 1662–1677
34. Zhou Y, Mumtaz MA, Zhang YH, Shu HY, Hao YY, Lu X, Cheng SH, Zhu GP, Wang ZW (2022) Response of anthocyanin accumulation in pepper (*Capsicum annuum*) fruit to light days. Int J Mol Sci 23: 8357

Figures

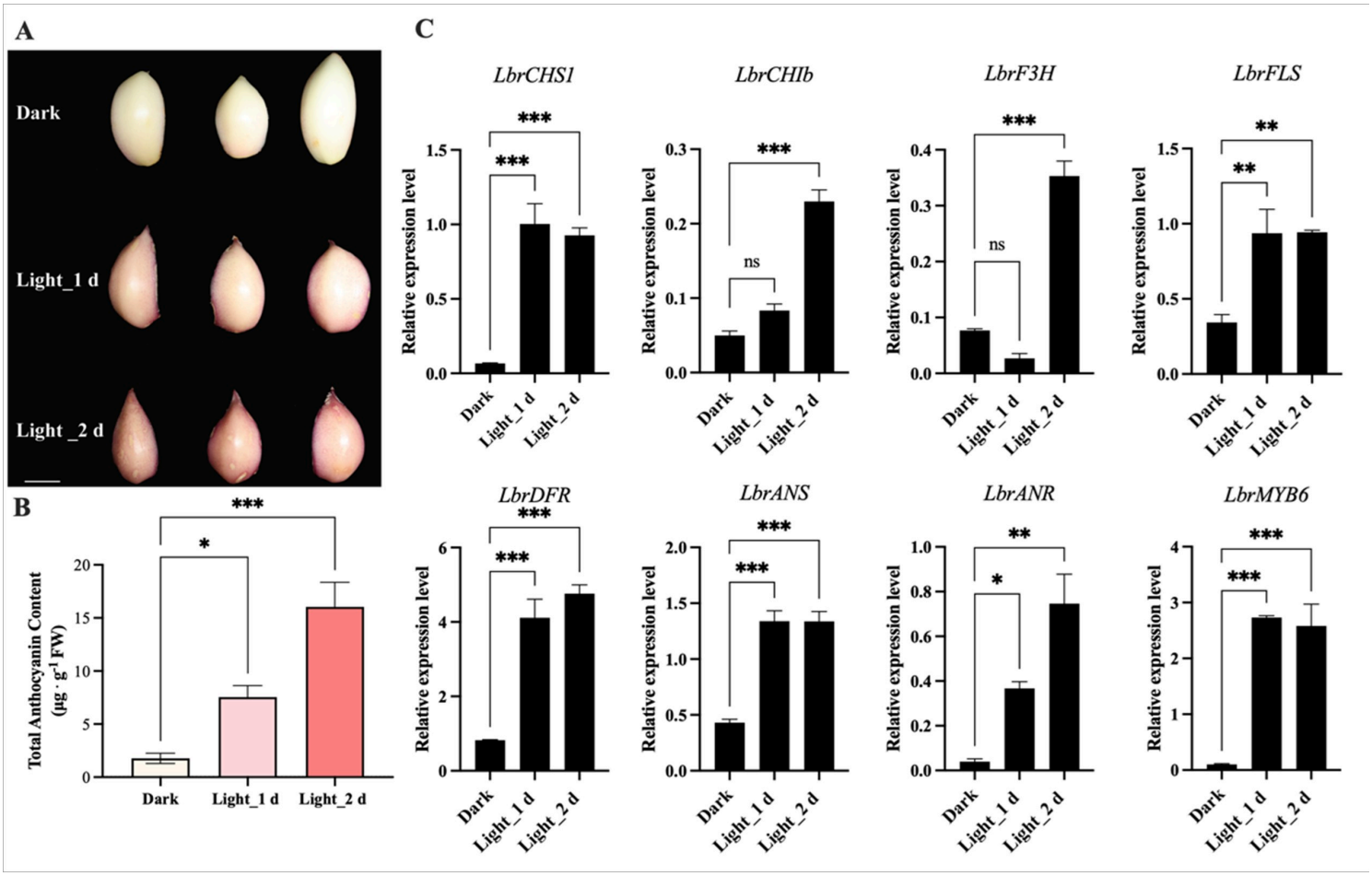

Figure 1

Total anthocyanin content and related gene expression in *L. brownii* following different light treatments. (A) Phenotypes of scales under different light conditions. Scale bar, 1 cm. (B) Total anthocyanin contents after light treatments. (C) Expression levels of genes related to anthocyanin biosynthesis after light

treatments. Gene expression was normalized to the internal reference gene, and relative expression levels were calculated using the $2^{-\Delta Ct}$ method. Data are presented as the means ± SEM (n = 3). Statistically significant differences were determined by ordinary one-way ANOVA followed by Dunnett's *t*-test (* $p < 0.05$, ** $p < 0.01$, *** $p < 0.001$, ns: not significant).

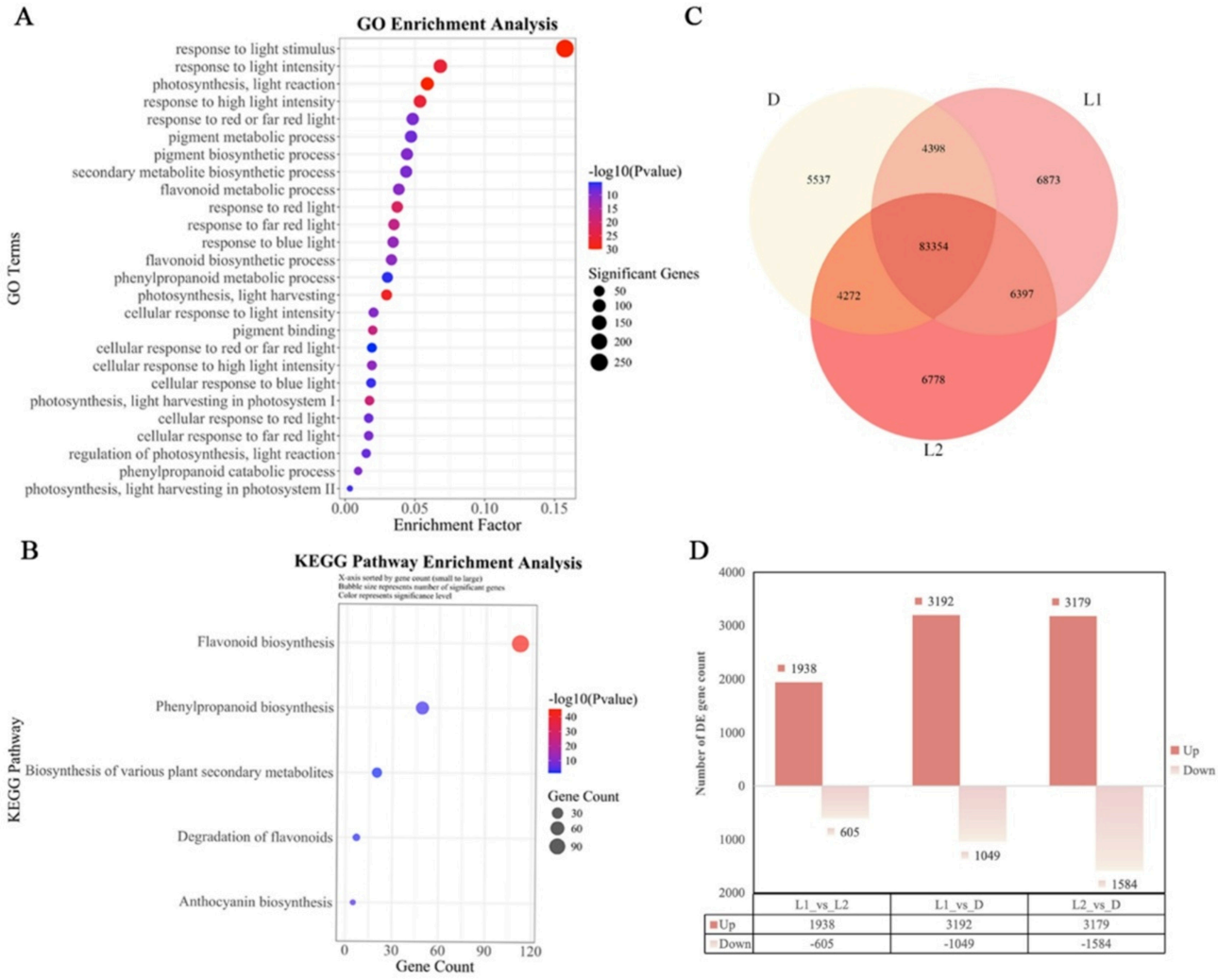

Figure 2

Transcriptome analysis of *L. brownii* scales exposed to darkness (D), 1 day of light (L1), and 2 days of light (L2). (A) Enriched GO terms related to anthocyanin biosynthesis and light among differentially expressed genes (DEGs) in the D, L1, and L2 groups. (B) Enriched KEGG pathways related to anthocyanin biosynthesis among DEGs in the D, L1, and L2 groups. (C) Venn diagram of the overlapping DEGs among the three groups. (D) Results of the statistical analysis of upregulated and downregulated genes in the three groups.

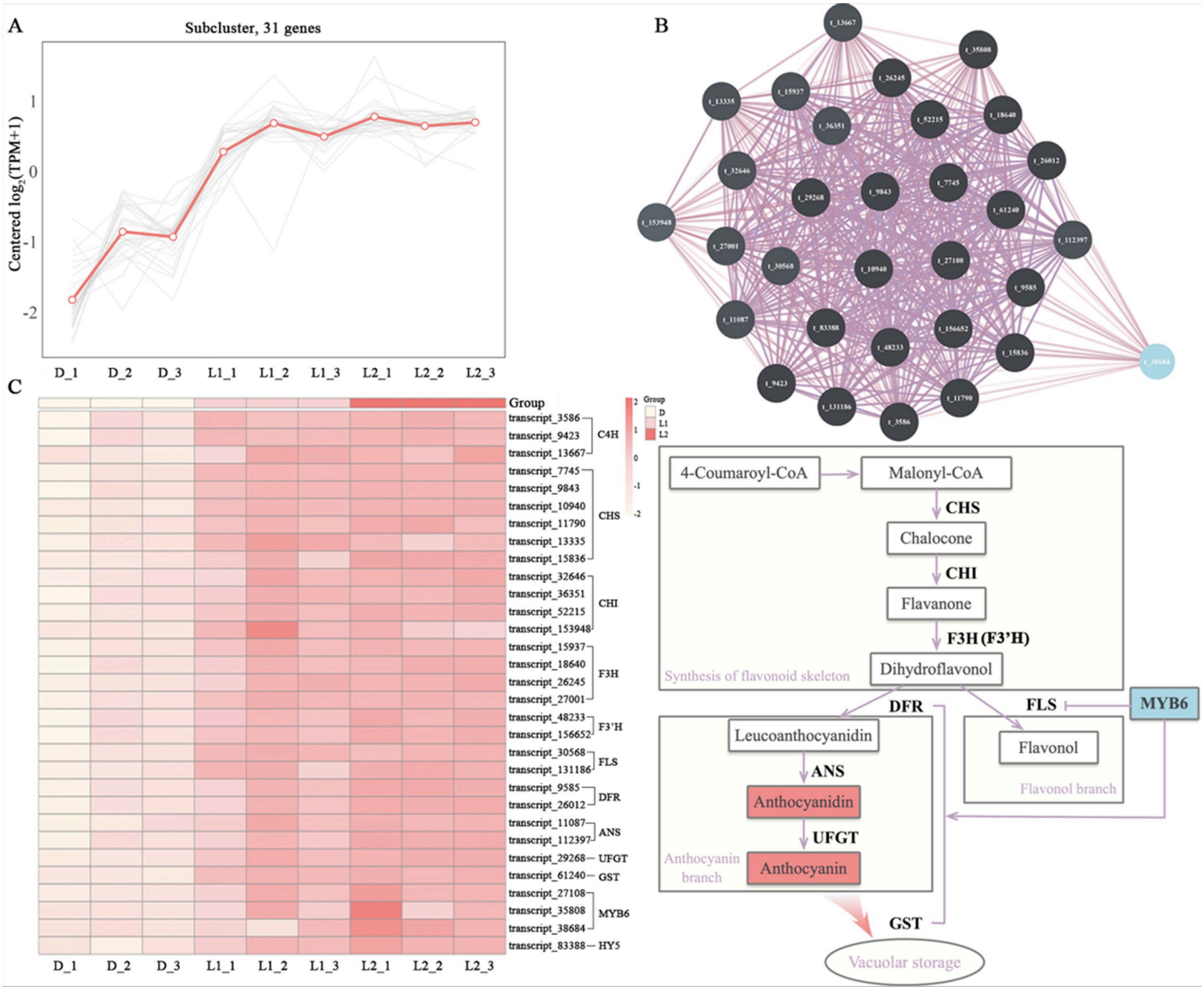

Figure 3

Analysis of differentially expressed genes (DEGs) among D, L1, and L2. (A) Subcluster matrix presenting the expression trends of 31 anthocyanin-related DEGs. (B) Co-expression network of anthocyanin-related DEGs. Relationship threshold <0.6. (C) Cluster heatmap of 31 DEGs related to the anthocyanin biosynthesis and regulatory pathway.

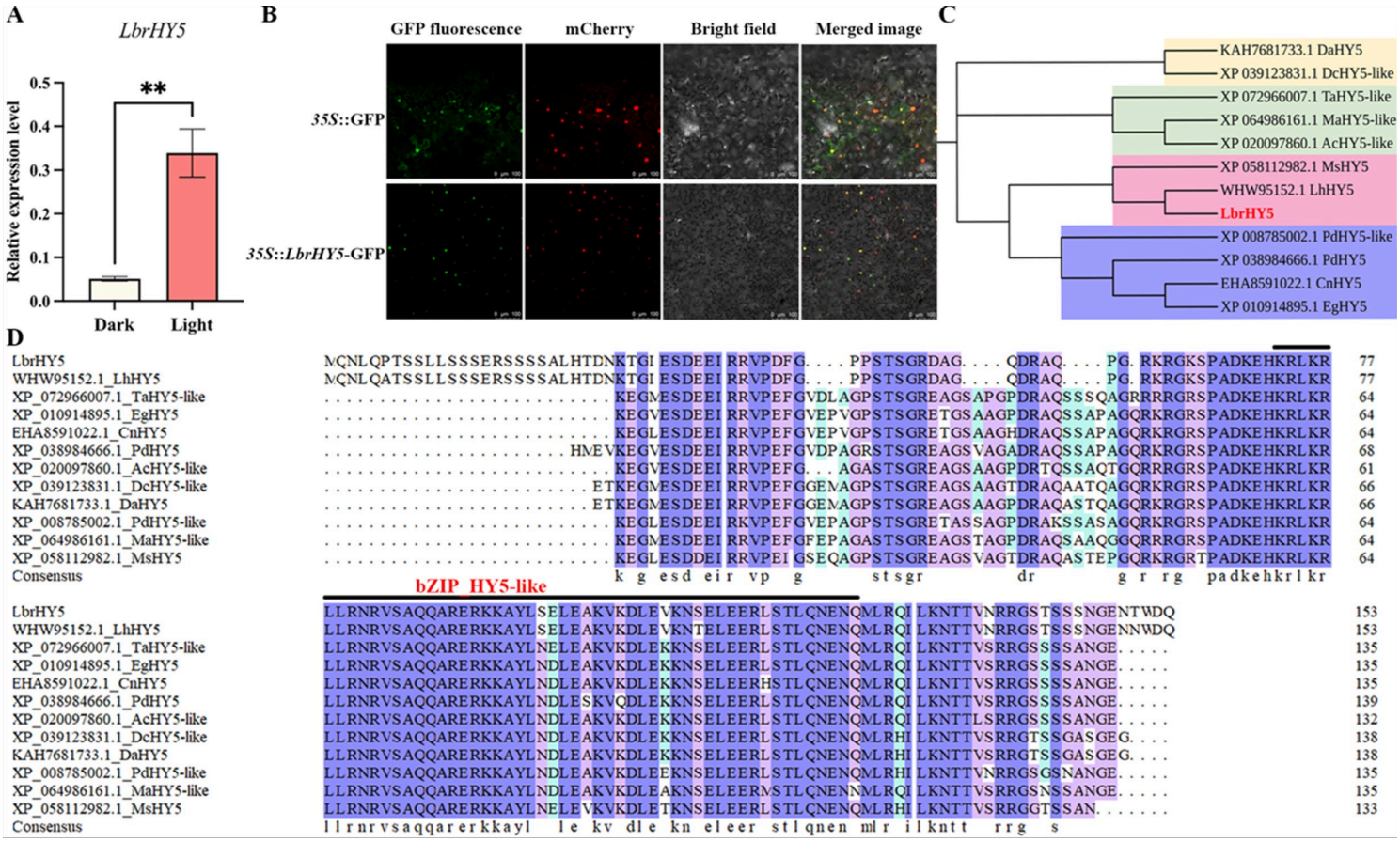

Figure 4

Bioinformatics analysis of LbrHY5 in lily. (A) *LbrHY5*expression levels in darkness and under light. Scales were treated with darkness (D) or continuous light for 2 days (L2). Data are presented as the mean ± SEM (n = 3). Statistically significant differences were determined using Student's *t*-test (** $p < 0.01$). (B) Subcellular localization of the LbrHY5-GFP fusion protein, with GFP alone used as a negative control. Bar, 100 μm. (C) Neighbor-joining phylogenetic tree derived from deduced amino acid sequences of LbrHY5 and other reported HY5s. Numbers next to nodes are bootstrap values from 1,000 replications. Amino acid sequences were retrieved from GenBank databases. (D) Amino acid sequence alignment of LbrHY5 and other reported HY5s. The bZIP HY5-like domain is indicated by a black line.

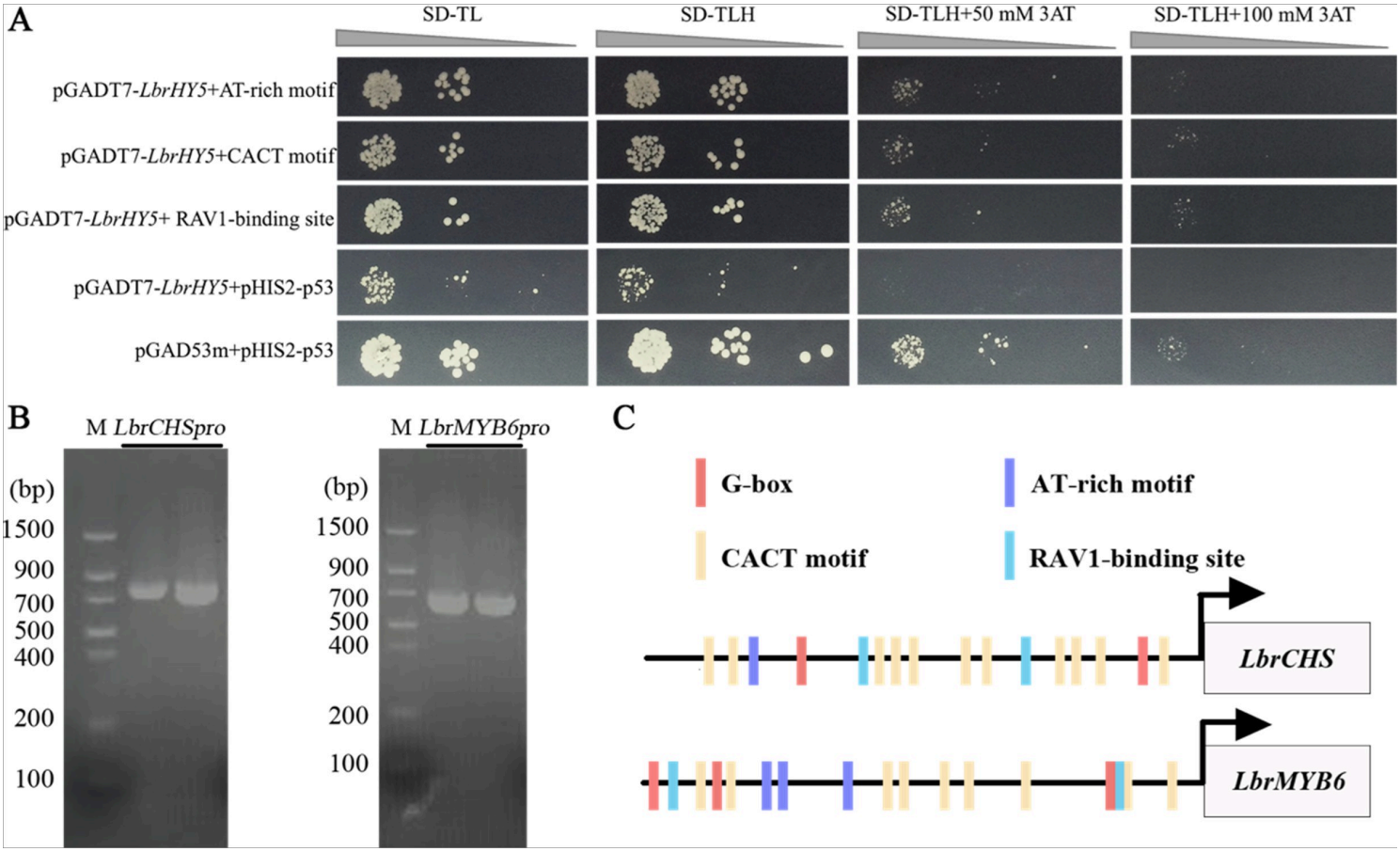

Figure 5

LbrHY5 can bind to multiple types of *cis*-elements in *LbrCHS* and *LbrMYB6* promoters. (A) Y1H assay results showing that LbrHY5 can bind to multiple types of *cis*-elements. (B) Genome walking-based cloning of *LbrCHS*and *LbrMYB6* gene promoters. (C) Identified *cis*-elements in *LbrCHS*and *LbrMYB6* promoters.

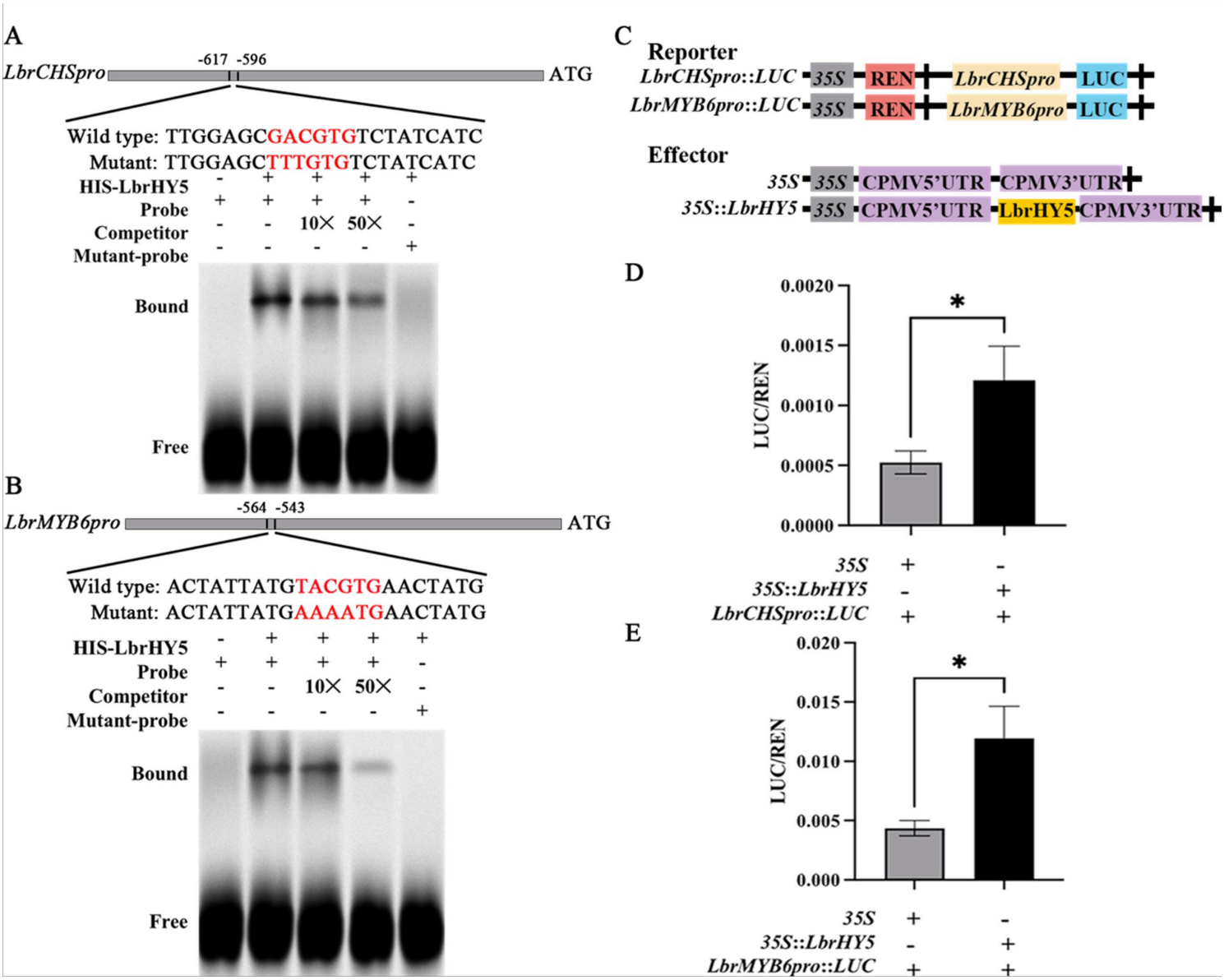

Figure 6

LbrHY5 can directly bind to *LbrCHS* and *LbrMYB6* promoters. (A) EMSA showing the binding of LbrHY5 to *LbrCHS* promoter fragments containing the G-box element. Unlabeled probes were used for the competition assay. (B) EMSA showing the binding of LbrHY5 to *LbrMYB6* promoter fragments containing the G-box element. Unlabeled probes were used for the competition assay. The G-box motif and mutant site are indicated in red fonts. + and - represent presence and absence of the protein and probe, respectively. Arrows indicated the positions of protein–DNA complexes for the free probe. (C) Schematic representation of the luciferase reporter vectors containing the *LbrCHS* or *LbrMYB6* promoters as well as the effector vector containing *LbrHY5*. (D) Dual-luciferase reporter assay showing LbrHY5 is a transcription factor that can activate the transcription of the *LbrCHS*. (E) Dual-luciferase reporter assay showing LbrHY5 is a transcription factor that can activate the transcription of the *LbrMYB6*. Each experiment was performed using 10 biological replicates. Data are presented as the mean ± SEM (n = 10). Significant differences were determined by Student's *t*-test at $p < 0.05$.

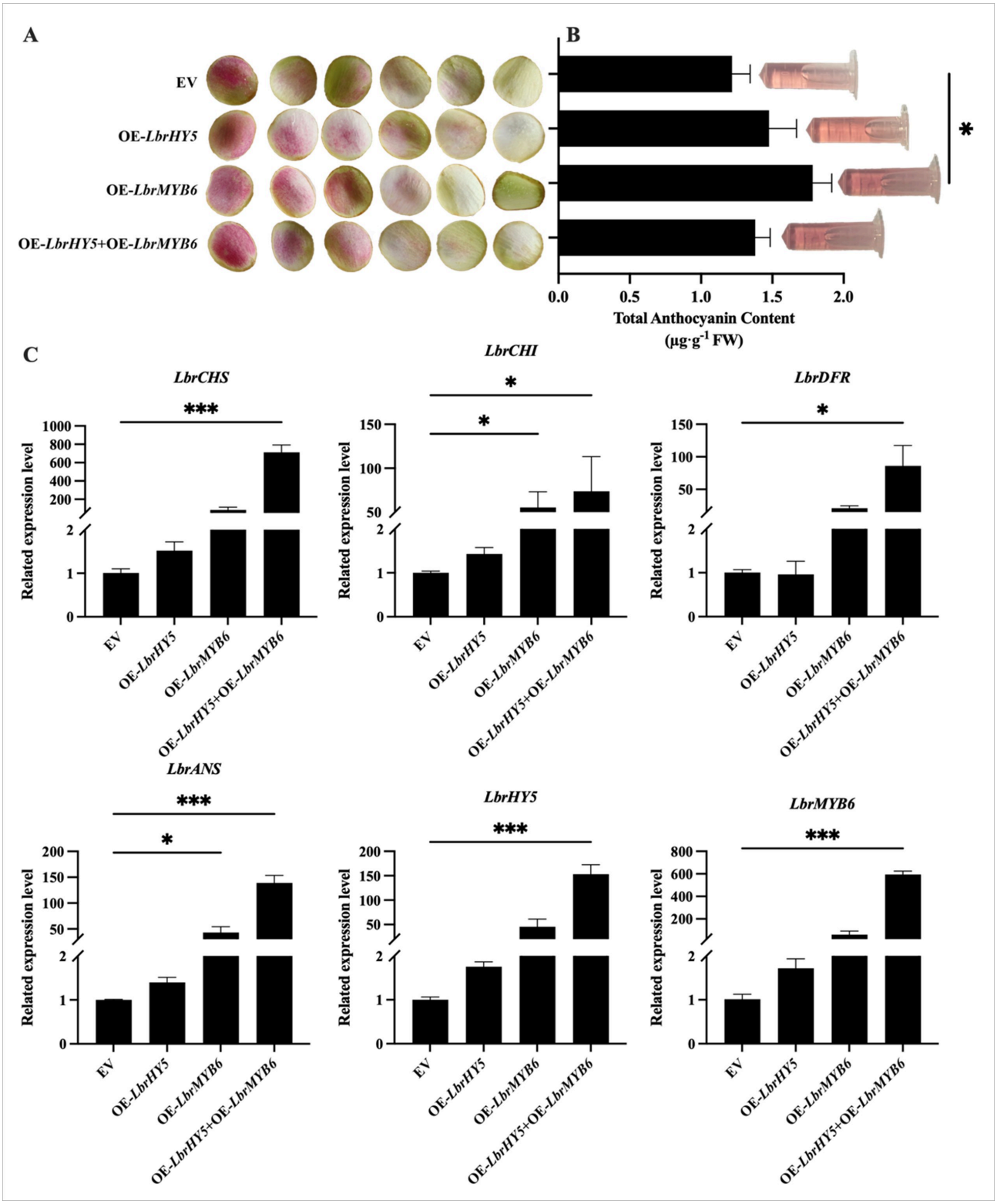

Figure 7

Phenotype and anthocyanin-related gene expression levels of 'Robina' tepals overexpressing *LbrHY5* (OE-*LbrHY5*), overexpressing *LbrMYB6* (OE-*LbrMYB6*) and co-overexpressing both *LbrHY5* and *LbrMYB6* (OE-*LbrHY5*+OE-*LbrMYB6*). (A) Phenotypic comparison of empty vector (EV) control tepals and overexpressing transgenic tepals. (B) Total anthocyanin contents of EV and overexpressing transgenic tepals. Three biological replicates were used for each sample. (C) Differences in the expression of

structural and regulatory genes related to anthocyanin biosynthesis between EV and overexpressing plants as determined by qRT-PCR. Gene expression was normalized to the internal reference gene, and relative expression levels were calculated using the $2^{-\Delta\Delta Ct}$ method, with the empty vector (EV) control group set to 1. Data are presented as the mean ± SEM of three replicates. Significant differences were determined by ordinary one-way ANOVA followed by Dunnett's multiple comparisonstest (* $p < 0.05$, ** $p < 0.01$, *** $p < 0.001$).

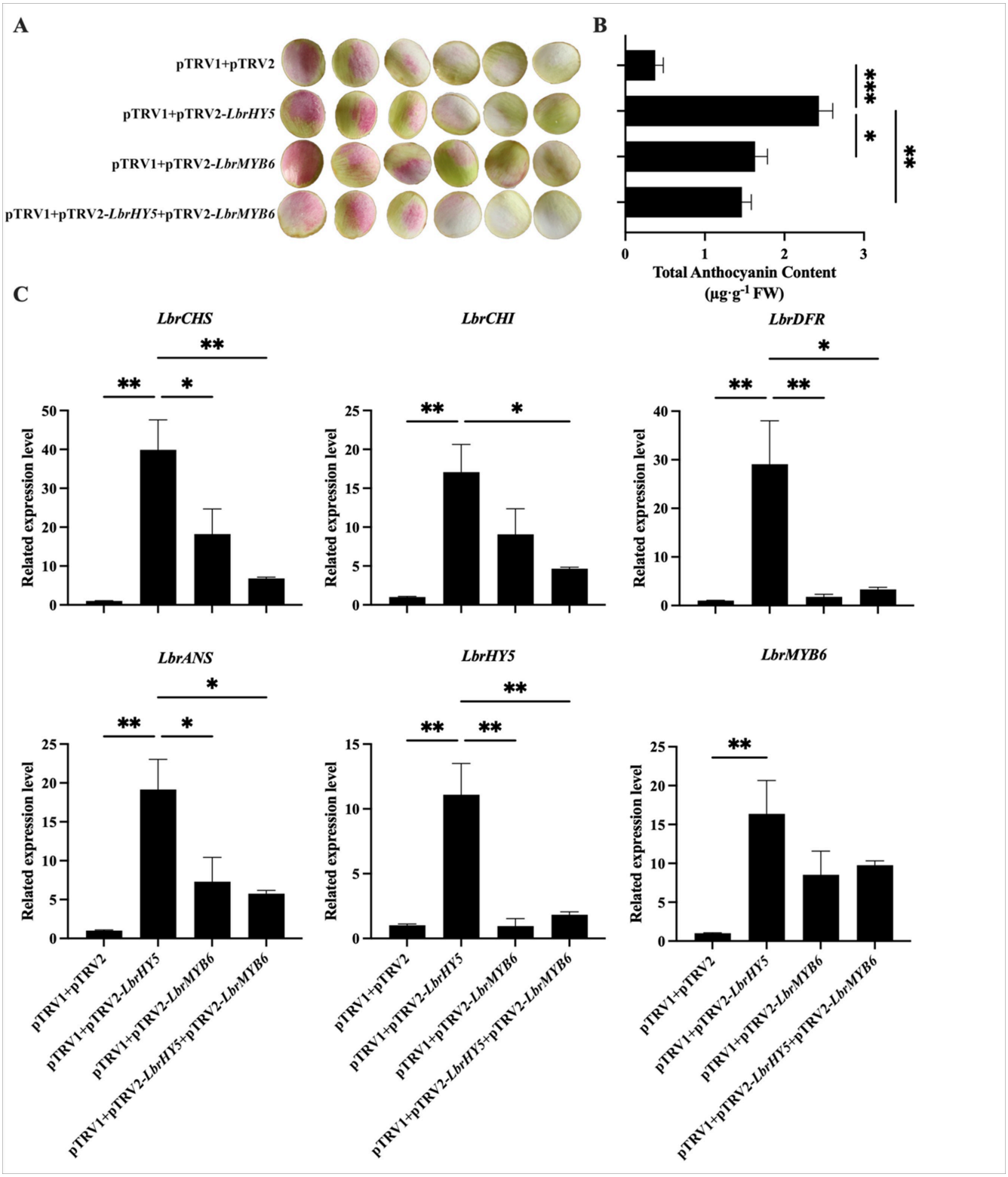

Figure 8

VIGS assay reveals the roles of *LbrHY5* and *LbrMYB6* in anthocyanin biosynthesis of 'Robina' lily. (A) Visual phenotypes of tepals following VIGS treatment with empty vector (pTRV1+pTRV2), pTRV1+pTRV2-*LbrHY5*, pTRV1+pTRV2-*LbrMYB6*, or their combination (pTRV1+pTRV2-*LbrHY5*+pTRV2-*LbrMYB6*). Tissues were harvested after 1-day dark incubation and 2 days under light. (B) Quantification of total anthocyanin contents in the treated tepals (mean ± SEM, n = 3). (C) Transcript levels of key anthocyanin pathway genes measured by qRT-PCR. Gene expression was normalized to the internal reference gene, and relative expression levels were calculated using the $2^{-\Delta\Delta Ct}$ method, with the empty vector (EV) control group set to 1. Data are shown as mean ± SEM (n=3). Statistically significant differences were determined by ordinary one-way ANOVA followed by Dunnett's multiple comparisons test (*$p < 0.05$, **$p < 0.01$, *** $p < 0.001$) compared to EV control (ordinary one-way ANOVA followed by Dunnett's multiple comparisons test).

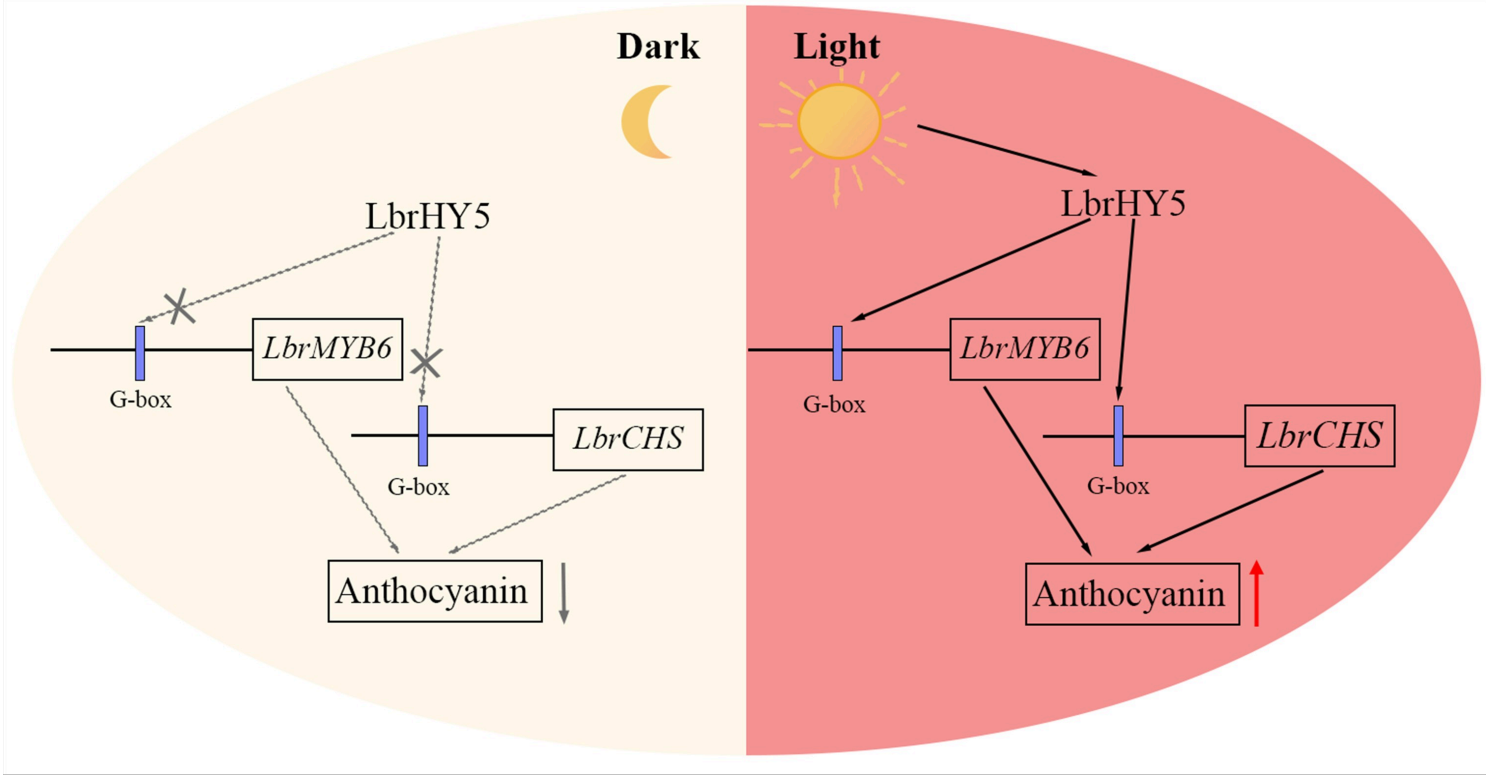

Figure 9

Working model for the effects of *L. brownii* LbrHY5 on anthocyanin biosynthesis in darkness and under light.

Supplementary Files

This is a list of supplementary files associated with this preprint. Click to download.

- Fig.S1.png

- Fig.S2.png
- TableS1.xlsx
- AppendixA.Supplementarydata.docx